Kashf Journal of Multidisciplinary Research
Vol: 03 - Issue 01 (2026)
P-ISSN: 3007-1992 E-ISSN: 3007-200X
https://kjmr.com.pk

MATHEMATICAL MODELLING OF NEWTONIAN FLUIDS FLOW PHENOMENA THROUGH DIFFERENT RATIOS OF BACKWARD STEP DUCT

Mazhar Ali Sahito[1], Akhlaque Ahmed Abbasi[2], Murteza Hussain Shar[3], Raunaque Ali Rid[4]
[1, 2]*Govt. Degree College Kandiaro.*
[3]*Govt Degree College Thari Mirwah*
[4]*Government Degree College Choondiko*

[*]***Corresponding Author:*** (mzsahito@gmail.com)
DOI: (*https://doi.org/10.71146/kjmr818*)

Article Info

This article is an open access article distributed under the terms and conditions of the Creative Commons Attribution (CC BY) license https://creativecommons.org/licenses/by/4.0

Abstract

The COMSOL Multi Physics CFD package is chosen here to develop the numerical model called as Galerkin least square finite element method and compute the steady state solution of the governing equations such as continuity and momentum equations in Cartesian coordinates form. The Newtonian fluid transported into the backward step duct with different aspect ratios (1: 6 and 1: 12) and change in characteristics length to observe the streamline patterns of the velocity, vortex enhancement on the basis of fluid inertia and vortex intensity. The research problem has vast application in the field of industries particularly to design the shapes of the rectangular tanks and observe the flow phenomena either compressible (gases) or incompressible (liquids). The streamline patterns are observed on different Reynolds number (01 to 600) and various ratios (1:6 and 1:12) of the backward step duct. Two vortices primary (lower left corner) and secondary (upper right corner) are visualized at various Reynolds numbers. At low Reynolds number (01), only primary vortex observed at the left lower corner of the backward step duct in both ratios. But due to growing Reynolds number, the primary vortex is increased largely in size but the secondary vortex increased also but very slowly in size. The primary vortex size is highly observed in the left lower silent corner of the backward step duct in the ratio 1:12 other than the ratio 1:6. Also, vortex intensity and vortex lengths plots justified the same enhancement due to growing the Reynolds number. Further, computed the empirical equations on the vortex intensity with various Reynolds numbers. The numerical results are compared with the available mathematical solutions by the use of CFD packages such as Flow 3D, ANSYS and others.

INTRODUCTION

The numerical simulation by the use of Computational fluid Dynamics (CFD) package of the fluid flow phenomena through backward step duct are preformed to observe the behavior of the fluids with change in the fluid inertia. The domain backward step duct relates to the various engineering and industries particularly focused on the designs of the water bottle industries, automotive large vehicles industries such as to design the silencer or muffler used in the heavy sports vehicles. Also, the domain transmits to the overhead airfoils, sections turbine blades and in large passenger automotive vehicles industries. The problem has vast applications in engineering such as tank filling and draining mixing, tank washing and store the chemical in a tank to transport into various routes of the water and other chemical flows (Camnasio, et al. [2013], Dufresne, et al. [2011], Siebert and Fodor [2009] and Pozrikidis [2009]).

Camnasio, et al. [2013] was adopted the flow model as depth average through computational fluid dynamics (CFD) package WOLF 2D for the investigation of the turbulence flow and sedimentation patterns of the velocity through the rectangular shallow type reservoir. The inlet and outlet were fixed at different locations of the domain to visualize the different flow patterns of the velocity and the k-□ model for the turbulent study was implemented. Also, the experimental method as laser light method was applied to compute the thickness of the sediments and observe the clean water flows. The velocity profile, various flow patterns of the velocity due to change the location of inlet and outlet and presence and absence of the sediments were examined. The all prediction of the velocity flow patterns were obtained accurately with comparison the experimental method as laser light method and suggested to change the numerical technique large eddy simulation for better results of the flow patterns.
Dufresne, et al. [2011] was investigated the symmetric and asymmetric fluid flow patterns through the two– dimension shallow reservoir expansion channel with influence of the aspect ratio (0.89, 1.25 and 4.38) of expansion reservoir and change in dimension length. The finite volume process was selected for the numerical solution with addition of CFD package WOLF 2D of the shallow water governing equations and some experimental tests were observed see Dufresne, et al. (2010). The predicted results were compared with the limited results of experimental results and achieved the good accuracy. Therefore, extended the flow patterns of the velocity with change small ratio into large aspect ratios and dimension length by use of CFD package WOLF 2D because the reattachment length of the vortex did not appear in the downstream of the expansion reservoir.

After the detail study of the research problems and found a different gap in numerical methodology and domain ratio and domain characteristics. The research problem is chosen here to adopt the computer simulation of Newtonian fluids through backward step duct with various large aspect ratios 1: 6 and 1:12. The finite element method is selected with coupling a Galerkin least square approach to compute the streamline patterns of the velocity, reattachment length of the eddies and recirculation flow of the small and large eddies in terms of the small and large Reynolds numbers. The all-predicted results are based upon the most advanced CFD package COMSOL MultiPhysics..

1.1 OBJECTIVES OF LITERATURE REVIEW

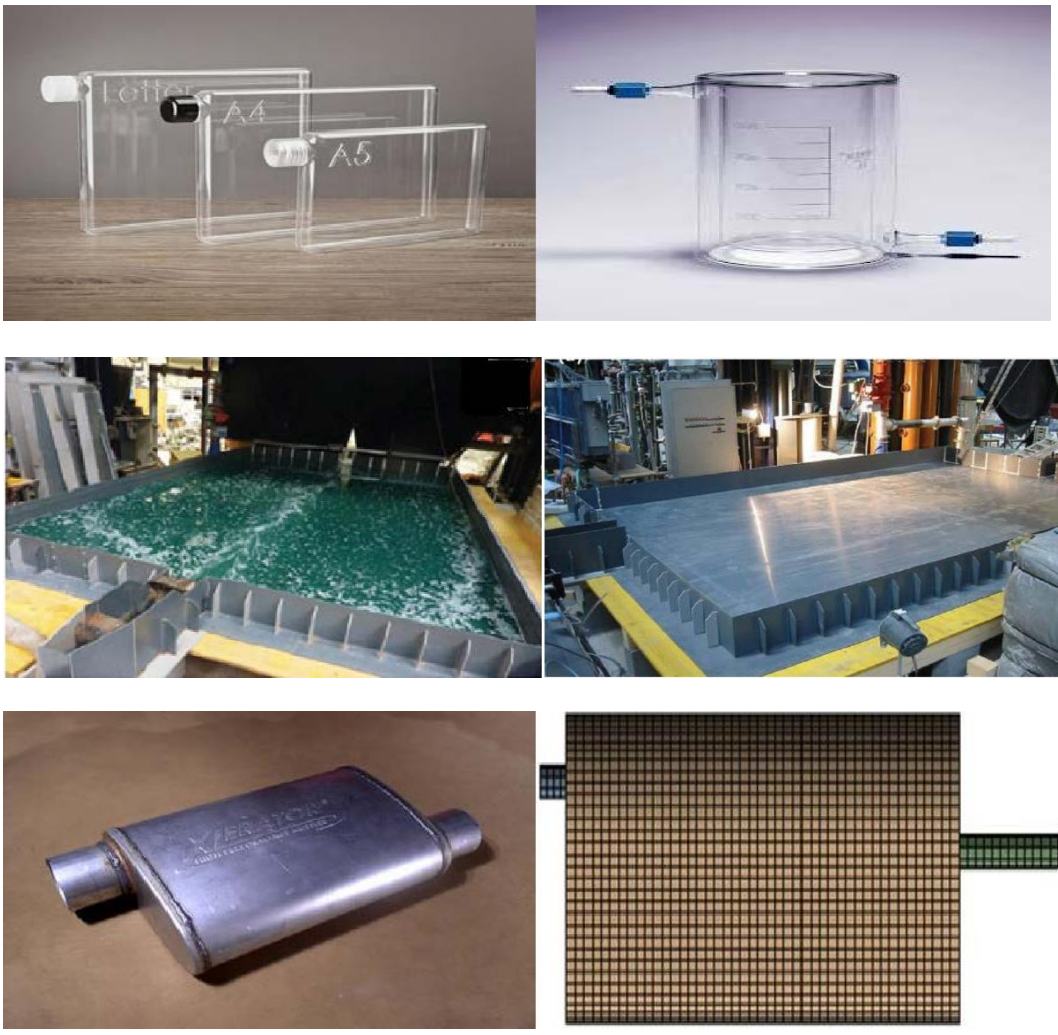

Figure – 1.1: Turbine blades fixed in the aircrafts and CFD simulations of bicycle seat.

That is focused on the study of the mathematical theory about the equations especially partial differential equations and the use in the field of the Computational Fluid Dynamics. This field is widely applicable by the addition of the mathematical and physical equations with the well-known predicted tools for the discretization process like Galerkin or Petrov–Galerkin finite element process. These discretization's may be obtained with the study of the CFD packages because CFD packages are highly used in the literature. For the continuity justification, needs a literature about the closed bodies of the real-life problems such as vessels, arteries, channels, ducts and so many.

1.1.2 BACKGROUND OF THE LITERATURE

Kantoush, et al. [2003] was tested and examined shallow water flows through the reservoir because of the most challenging research problem of low velocity and water depth flow field through experimental setup. Also, predicted the flow patterns through the finite element-based package CCHE2D and this package was also employed for the shallow water modeling through the open and closed bodies. The various studies were focused in this research like impact of the geometry like reservoir with and without sediment filling the deposition. For the experimentally. Heavy equipped machinery and heavy expensive instruments was fixed such as Large-Scale Particle Image Velocimetry (LSPIV) and Ultrasonic Doppler Velocity Profiler (UVP). Various studies were discussed as influences of the vertical velocity field, compared all experimental tests with the numerical tools through shallow sediments via two predicted model Large-Scale Particle Velocimetr (LSPIV) and (UVP). In the last, the model LSPIV competency was justified the velocity computations exposes clearly at low velocity of the shallow water but felt some difficulties in the numerical modelling through the package CCHE2D.

Dufresne, et al. [2011] was investigated the experimental tests for the development of the shallow water flow patterns, sediment depositions and tested the deceiving productivity through the different shapes of the reservoir geometry with change in the ratio of the width. The reservoir related to the expansion channel with fixed inlet and outlet small channels in the center of the body. Different phenomenon of the eddy's appearance observed such as symmetric flow features in the absence of the eddy, asymmetric flow features in the presence of the single and double eddies. The electromagnetic flow meter was fixed to compute the flow rate through the fixation of the metallic flume in the reservoir. The flow patterns and sediment depositions results was based upon the different non–dimensional numbers of the physical phenomena like Reynolds number, Froude number, bed friction number and change in water depth of the reservoir. It was results that the asymmetric flow features observed in all sediment deposition tests and found that shape parameter in a reservoir was greater than 6.8 was better in the deposition of the sediments other than the 6.2 limit of the sediments deposition in the reservoir domain.

Camnasio, et al. [2013] was studied the velocity flow patterns and sediment patterns via a rectangular shallow reservoir. Two techniques were used as experimental through laser light method and package WOLD 2D through finite volume 2nd order discretization includes with mean k-□ turbulent model. The predictions were computed for develop a velocity profile and different flow patterns on the bases of the sediment deposits. These problems related to the urban hydraulic structures and used for the analyzed the design of

the reservoir and preserve the man – made materials for example storm tanks or basins. The conclusions were described the flow patterns was observed in the reservoir with reattachment of the eddies at the left silent corner and due to the filling, the sediments, the flow patterns and eddies diminished completely with filling the 30min supply of the sediments in the reservoir. The stable predicted results through the package were validated with the experimental results through different tests of the filling sediments in the reservoir.

Tarpagkou and Pantokratoras [2013] was extended the asymmetric flow patterns through the 3D tank filled with the sediment and the tank relates to the duct type with inlet and outlet at the center. The limited experimental test was carried out but the full simulation of turbulent flow patterns like velocity vectors, streamline patterns, reattachment length of upper and lower eddies was adopted through the

CFD package Fluent. The Fluent was based upon the finite volume too with SIMPLE discretization process to compute pressure and velocity through couple Navier–Stokes equations. Most stabilized model of turbulent flow phenomena was adopted like renormalization group k-ε model that was better than the simple k-ε turbulent model. The single phase (water), two phase (water with solid particles) change were employed in the tank on the variety of the physical non –dimensional numbers such as influence of the Reynolds number and Froude Numbers. At last, the recirculation vortices occupied the whole area of the tank due to low volume of the particles of sediments but due to increase the particle size, the new small vortices appeared at the outlet of the tank.

Tutunea, et al. [2013] was also simulated the ideal gas flows through the CFD development design of the silencer by the use of the heavy computational setup. The silencer modelling was highly adopted in the field of the aerodynamics and vehicle industries. The computational setup was fixed to design the schematic diagram, unstructured mesh setup and was presented the streamline of the velocity, pressure contours, Vorticity that based upon the density and Mach number. Through CFD modelling, examined the pressure falls, minimize and maximize the temperature and controlled the noise pollution. These mufflers were activated through the acoustic modelling for the energy creation and added the different materials like porous and fires. In the last, validated that CFD package was better agreement than analytical lengthy techniques and heavy expensive experimental setup in the vehicle industries.

Choufi, et al. [2014] was developed the experimental modelling about the sedimentation in the reservoir that was complex problem in the field. The experimental image process through the large-scale particle image tool was employed to compute the ultrasonic velocity profile. The rectangular channel was assumed for the reservoir modelling to examine the controlling and decreased sediment in the reservoir and also analyzed the surface roughness influences through shallow reservoir. In the start, asymmetric flow patterns were observed on the symmetric boundary conditions and then the conditions were stabilized then found the symmetric recirculation flow rate at limited turbulent flow conditions. Different flow contours were examined like velocity distributions, boundary layer at bottom of the reservoir with the influence of the different values of the Reynolds number and various values of the viscosity of the fluids. It was resulted the flow patterns found asymmetric after the boundary conditions are fully symmetric fixed at the ones of the two–dimensional rectangular basins.

Saripalli and Sankaranarayana [2015] were designed the CFD based muffler in the shape of the rectangular tank. For CFD based muffler was developed through the CATIA package and then for the flow analyzed chosen the ANSYS Fluent package. The muffler fitted in the large vehicles and pollution had and has large problems in the environment and the design related to the automotive industries and through CFD packages, easily designed the shape of the muffler and examined the improvement the performance of mufflers fitted in the engines. Also, investigated the pressure variations, velocity, magnitudes and contours in the mufflers and analyzed the pressure drop to extend the muffler designs modifications. The same muffler fitted in the experimental laboratories and proved that the muffler setup in CFD was better analyzes for improvement the shapes and pressure drop predictions. Two models of muffler circular and rectangular were designed to compute the velocity field and pressure drop and it was concluded that the second design performance was better than the first due to exhaust pressure drop.

Trivedi, et al. [2017] was studied the gases flows through the different type of silencer geometries and examined the pressure falls and controlled the temperature decreased in the exhaustive system. The

study based upon the numerical predictions through the CFD package ANSYS Fluent. The silencer geometry related to the rectangular tanks and reservoirs and it is main part of the exhaustive system and used for control the noise system and decreased the temperature and pressure variations. Various form of the geometries circular and rectangular type with different ratios were designed with suitable mesh designing through the mathematical conservative equations. The velocity contours, velocity magnitudes, pressure contours and temperature drops. Also, designed the experimental setup to validate the gas flows through the fixation a silencer in the automotive vehicles and found good agreement in between real gas flows through silencer experimentally and numerically. In the last, the curved outlet boundaries-based silencer geometry was recommended to minimize the pressure drop and increased the temperature drop after validation with experimental setup.

Westhoff, et al. [2018] was also discussed on the investigation of the analytical solution of the fluid motion equations that described the flow patterns through the shallow reservoir geometry that related to the rectangular duct. The symmetric and asymmetric flow patterns focused on eddies developments, recirculation's observed and energy dissipations. Two tanks with varying length were structured with triangular mesh styles and found the symmetric flow patterns in low length tanks but due to large length, asymmetric flow patterns observed and small and large eddies observed at the left corner of the tank or shallow reservoir. It was caused that symmetric vortices (jets) found in the lower tanks and asymmetric vortices (jets) observed in the lower and upper corner of the sediments tank and also energy dissipations were higher in the symmetric flow patterns and lower in the asymmetric flow patterns in vortices.

Miranda, et al. [2018] was consequently, modelled the flow patterns experimentally by the use of the full equip laboratory tests and numerical approach through the CFD package WOLD 2D. Separate flow behavior observed like symmetric and asymmetric patterns through the shallow reservoir with length 3.0 m and width 2.0 m and depth was 0.30 m. The main purpose of the research problem to examine flow patterns symmetrically situated in the upstream and downstream tanks with various flow rates and based upon the steady state flows. The shallow liquid (water) equations were selected through the CFD package WOLF 2D and computed the velocity profile through the turbulent k-□ model with the finite volume discretization's. It was resulted the flow features observed symmetric eddies in the corner experimentally in lower flow rates only but found asymmetric vortices in higher flow rate but in numerical modelling, only symmetric flow eddies observed in all flow rates lower and higher with all depths of the water through the shallow reservoir.

CFD MODELLING OF NAVIER – STOKES EQUATIONS THROUGH COMSOL MULTIPHYSICS PACKAGE

The Computational Fluid Dynamics (CFD) field is a new and vast applicable field because of the use of the Mathematical equations particularly, partial differential equations and the physical concept with the use of the computational machines to control the large solution of the problem. The problem related to the sciences, engineering and mostly industries like medical sciences, aerodynamics and hydraulic engineering and also vehicle industries. The CFD based upon the computational packages like ANSYS, COMSOL MultiPhysics, FlexPDE's and many more. Through these packages, the problem may be designed, discretized, computed and visualised through the closed and open bodies relates to the real-life problems. The most important, chosen the suitable numerical technique to control the steady state and transient phenomena of the fluid motion equations because every method have some limitations but may be quick and fast convergence. Due to the most important and vast applicable in the field, chosen here finite element technique through the use of the COMSOL MultiPhysics. (Tutunea, et al. [2013], Trivedi, et al. [2017] and Memon, et al. [2018]).

The COMSOL MultiPhysics package is based upon the finite element mathematical tool and consisted the vast applications with the use of the computational algorithms and required termination level of accuracy.

Figure – 3.1: Flow chart of the COMSOL MultiPhysics

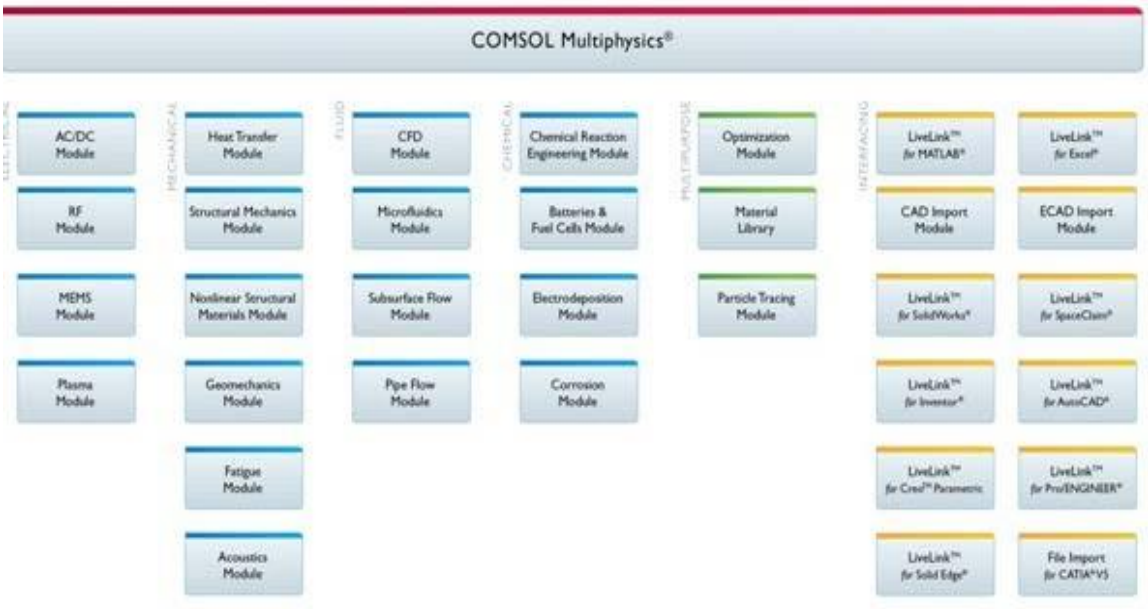

The package has vast flow chart in which chosen a laminar flow problems and then chosen the governing equations of fluid dynamics that are built-in and discretized through various finite element schemes like Galekrin and Petrov–Galerkin and many more. Initially, discussed the governing equations relates to the research problem in this project.

1.1 THEORY OF GOVERNING EQUATIONS

The theory of governing equations is focused on the conservative laws of Physics that is called as conservative law of mass and other is momentum. These laws are described here continuity and momentum transport equations in two–dimension and in Cartesian

Coordinates due to the domain based upon the rectangular channel. These equations are limited for the Newtonian and incompressible fluids for the coupling of the velocity field and pressure.

1.1.1 EQUATION OF CONTINUITY

This equation is used here for the continuum assumption that the rate of the fluids transported at the inlet of the body must be equal rate of fluids outflows at the outlet of the body. This assumption is described here Mathematically in two – dimension and for incompressible fluids only because of the domain of interest.;

For Incompressible fluids

$$\frac{\partial u^*}{\partial x^*} + \frac{\partial v^*}{\partial y^*} = 0 \qquad (3\text{–}1)$$

Here u and v show the vector velocity field and known as divergence free vector.

1.1.2 EQUATIONFOR MOMENTUM TRANSPORT

The equations are used here the how momentum transported with the coupling of the external forces like pressure. This equation is resulted from the most popular law of mechanics called as Newton's second law of motion and is described as the force is directly proportional to acceleration of the body and is listed as under;

$$F = m\ a \qquad (3-2)$$

Where F shows the external force, a show the acceleration of the body and m shows the proportionality constant. The equation (3 – 2) can be differentiated with the addition of the physical properties of the fluids called as density, viscosity, vector velocity field and pressure and many other terms of the fluid dynamics. The general form of the momentum transport equations in dimension form is described as under;

$$\rho(\mathbf{u}.\nabla)\mathbf{u} = \nabla\left[-pI + \mu\left(\nabla\boldsymbol{u} + (\nabla\boldsymbol{u})^T\right)\right] + F \qquad (3\text{–}3)$$

The equation (3 – 3) is based upon the various type of fluids and many kinds of flow phenomena but due to limitation of the research problem. The equations are stated for the laminar flow of Newtonian liquid flows and in two–dimension. The following equations are discussed here in the non – dimension form for the quick solution and for simplicity. So removed the physical properties like viscosity and density and can be converted into the non – dimensional number known as Reynolds

number. This number is used for the fluid flow resistance and it is called the fluid inertia. The following equations are listed below for the limited research problem;

$$\frac{\partial u^*}{\partial t} + \left(u^* \frac{\partial u^*}{\partial x^*} + v^* \frac{\partial u^*}{\partial y^*} \right) = -\frac{\partial P^*}{\partial x^*} + \frac{1}{Re} \left[\frac{\partial}{\partial x^*} \left(\frac{\partial u^*}{\partial x^*} \right) + \frac{\partial}{\partial y^*} \left(\frac{\partial u^*}{\partial y^*} \right) \right] \quad (3\text{–}4a)$$

$$\frac{\partial v^*}{\partial t} + \left(u^* \frac{\partial v^*}{\partial x^*} + v^* \frac{\partial v^*}{\partial y^*} \right) = -\frac{\partial P^*}{\partial y^*} + \frac{1}{Re} \left[\frac{\partial}{\partial x^*} \left(\frac{\partial v^*}{\partial x^*} \right) + \frac{\partial}{\partial y^*} \left(\frac{\partial v^*}{\partial y^*} \right) \right] \quad (3\text{–}4b)$$

Here Re is known as fluid flow inertia or Reynolds number that is focused as below

$$Re = \frac{\rho \times u_{avg} \times L}{\mu}$$

Whilst, ρ stated as density of the fluid, μ stated as the viscosity of the fluid, L stated as the length of the channel and u_{mean} state as the average velocity.

1.1.3 FINITE ELEMENT METHOD

Historically, initially Richard Courant was provided this technique in the start of 1940 who was German and American mathematician this technique was used for the various problems relates to the structural mechanics and still employed this tool in same fiel

and now a day extended into the various other field of mechanics such as solid and fluid mechanics. FEM numerical tool makes the predicted solution not limited in the mechanics but it can be employed in other sciences like chemistry, Physics and particularly vast applications in the biological sciences. FEM tool can be described in different dimensions either 1D, 2D or 3D through the use of the CFD package COSMOL MultiPhysics. Some examples are as under.

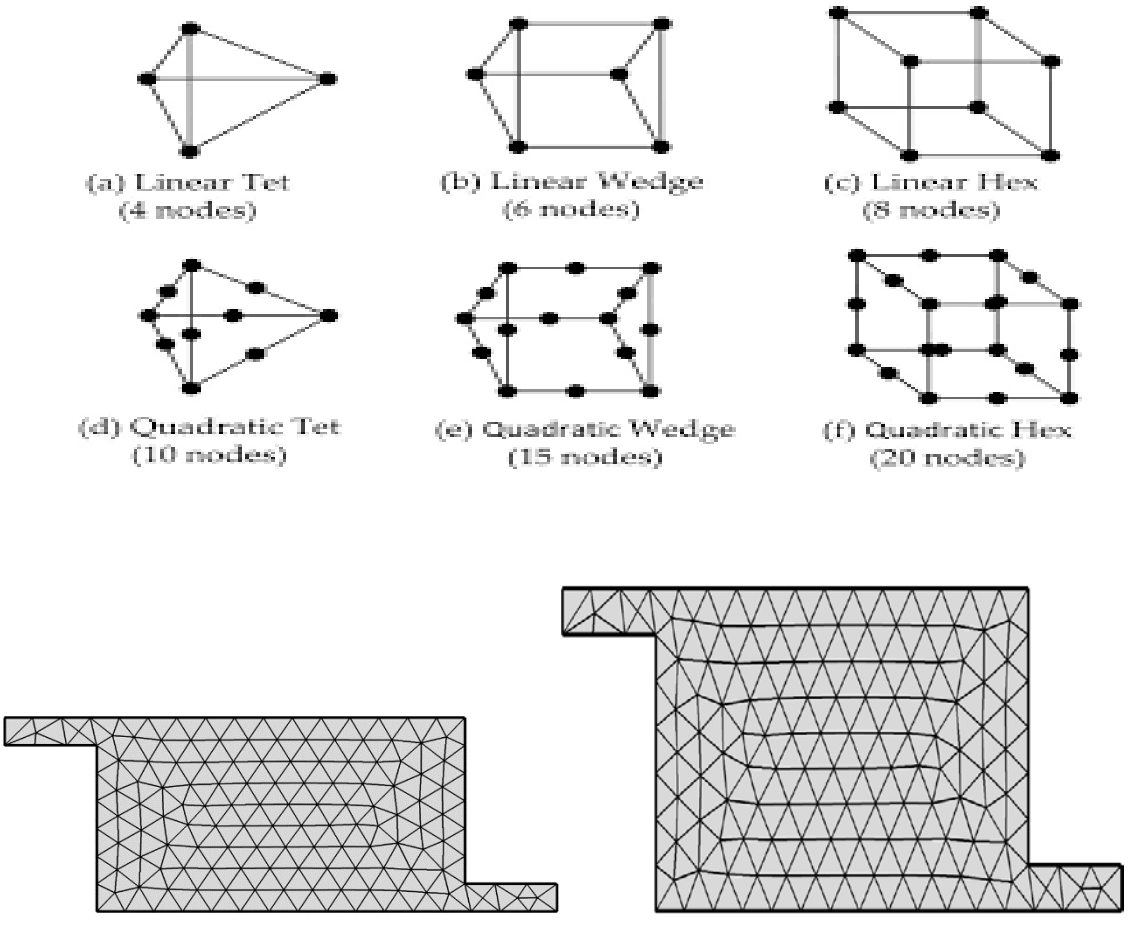

Figure – 3.2: various styles of the finite element discretization's

Above figure – 3.2 displays the various shapes elements. Edges, nodes and full faces of the domain.

By the use of the individual node, designed the set of discrete form equations after the conversion the derivatives into the small unknowns with required boundary value conditions.

The FEM is a numerical method and used to divide the whole complicated domain into the piece wise small elements that may be computed in relation to each other. The whole domain described the partial differential equations and the piece wise elements displays the simple algebraic terms derived from the discretization process of the FEM. FEM tool is widely adopted in the CFD packages like ANSYS CFX, COMSOL MultiPhysics, open Foam and many more. The use of FEM tool ranges more fields of physical and biological sciences and many industries. Such as vast usage in the designing of aircraft industry, electrical and most important computer industry. Now a day, FEM tool proved a most important tool in the manufacturing the medicines and whole in biosciences, especially, modelling needed the structure of tissues and FEM simulation needed in the modelling of the blood flow through arteries, bones and muscles and many more. Also, FEM proved the simulation and modelling is better than even experimental techniques.

Here FEM tool is employed due to large importance available in the literature and FEM tool is applied on the governing equations with the availability of the CFD package COMSOL MultiPhysics. Bu the packages consisted the various other schemes of FEM such as Galerkin and Petrov – Galerkin. Here chosen only Galerkin FEM and also added in the FEM, least square process to easily control the steady state solution of the governing equations.

1.1.3.1 GALERKIN LEAST SQUARE FINITE ELEMENT TECHNIQUE

The finite element process is widely used for the predicted solution of Navier–Stokes equations in the field of the CFD, especially for the Partial differential equations. Also, so many other predicted methods like finite volume and boundary value method and lattice Boltzmann method have been employed through the computational language coding and many more employed with the developed CFD packages. Basically, designed the FEM individual model for the elasticity problems in the field of the structural Mechanics and then fluid mechanics and many more. Here described the hybrid approach for the solution of PDEs such as finite element method with least square approach. LSGFEM is more reliable and motivated technique to cover all merits approaches of Rayleigh-Ritz methods especially handled the compatibility discrete conditions and removed the property of symmetry and also positive definite simple systems. This method is focused on the optimize the convex unknowns which are developed through system of equation residuals (Bochev and Gunzburger [2005]).

Mostly, LSGFEM may be defined standardly for the solution of PDE through forcibly pushing the residuals of the equation into the orthogonal towards the subspaces of the finite element. The finite element approach with addition of least square procedure have so many advantages practically such as bases are quickly developed for compatible subspaces, system especially linear are quickly constructed and system of linear are comparatively well posed. Also, LSGFEM have many more advantages other than FEM method or Rayleigh-Ritz technique like least square residual delivered certainly solvable residual indicator error which may be employed for adjusting meshes. Consequently,

setup of the homogeneous or as well as non – homogenous boundary conditions residuals may be integrated towards least square unknowns.

The LSGFEM is a robust method and more easily computable the unknowns of the partial differential equations used for the Navier–Stokes problems in the field of the fluid mechanics and more reliable on the first order system of governing equations. Therefore, chosen the extra parameter Vorticity to be converted the 2nd order Navier–Stokes equations into the Vorticity velocity –pressure formulation. The Vorticity can be defined as $\boldsymbol{w} = \nabla \times \boldsymbol{u}$ and $\nabla \times \boldsymbol{u} = -\nabla^2 \boldsymbol{u}$ so that by using the procedure, can be shifted the higher order into the first order system that are highly useful and more reliable by the use of LSGFEM (Babuska, et al. [1972] and Bochev and Gunzburger [1994, 2005 a and b]).

1.1.3.2 PROCEDURE OF FIRST ORDER SYSTEM THROUGH LSGFEM

In the start, the problem chosen here the 2nd order momentum equation with continuity equation but the numerical tool chosen here least square Galerkin FEM and it is applicable only on the first order system of equations. Therefore, it is essential to describe any algebraic process to remove higher order term in the momentum equation. Here added extra variable Vorticity known as curl of the velocity. The process is given as below;

$$\nabla . \boldsymbol{u} = 0 \tag{3 – 6}$$

$$-\frac{1}{\mathrm{Re}}\nabla^2 \boldsymbol{u} + \nabla P + \boldsymbol{u}(\nabla \boldsymbol{u}) = 0 \tag{3–7}$$

Now added extra parameter Vorticity that are

$$\boldsymbol{w} = \nabla \times \boldsymbol{u} \qquad (3-8)$$

As per identity of vector analysis, it is described as below;

$$\nabla \times (\nabla \times u) = -\nabla^2 .\mathrm{u} \qquad (3-9)$$

After the equations (3 – 8) and (3 – 9) substituted into the (3 – 7), the resulted the system described below;

$$\nabla . \boldsymbol{u} = 0 \qquad (3-10a)$$

$$\boldsymbol{u}.\nabla \boldsymbol{u} + \frac{1}{\mathrm{Re}} \nabla \times \boldsymbol{w} + \nabla p = 0 \qquad (3-10b)$$

$$w - \nabla \times \boldsymbol{u} = 0 \qquad (3-10c)$$

The required problem is two – dimensional and fluid is incompressible and Newtonian and described into the Cartesian Coordinates form as under;

$$\frac{\partial \mathrm{u}^*}{\partial x^*} + \frac{\partial \mathrm{v}^*}{\partial y^*} = 0 \qquad (3-11a)$$

$$u \frac{\partial u^*}{\partial x} + v \frac{\partial u^*}{\partial y} + \frac{\partial P}{\partial x} + \frac{1}{\mathrm{Re}} \frac{\partial w^*}{\partial y} = 0 \qquad (3-11b)$$

$$u \frac{\partial \mathrm{v}^*}{\partial x} + v \frac{\partial \mathrm{v}^*}{\partial y} + \frac{\partial P}{\partial y} - \frac{1}{\mathrm{Re}} \frac{\partial \mathrm{v}^*}{\partial x} = 0 \qquad (3-11c)$$

$$w^* + \frac{\partial u^*}{\partial y} - \frac{\partial v^*}{\partial x} = 0 \qquad (3-11d)$$

Now the system (3 – 11) is known as first order system, Further solution can be shifted into the matrix system of all unknowns (u, v, P and w) with respect to x and y.

$$A_1 = \begin{pmatrix} 1 & 0 & 0 & 0 \\ u & 0 & 1 & 0 \\ u & 0 & -1 & \frac{1}{Re} \\ 0 & 0 & \frac{1}{Re} & 0 \\ 0 & -1 & 0 & 0 \end{pmatrix}, \quad A_2 = \begin{pmatrix} 0 & 1 & 0 & 0 \\ v & 0 & 0 & \frac{1}{Re} \\ v & 1 & 0 & 0 \\ 1 & 0 & 0 & 0 \end{pmatrix}$$

$$A = \begin{pmatrix} 0 & 0 & 0 & 0 \\ 0 & 0 & 0 & 0 \\ 0 & 0 & 0 & 0 \\ 0 & 0 & 0 & 1 \end{pmatrix}, \quad f = \begin{pmatrix} 0 \\ 0 \\ 0 \\ 0 \end{pmatrix}, \quad \mathbf{u} = \begin{pmatrix} u \\ v \\ p \\ w \end{pmatrix}$$

Now apply the least square Galerkin FEM discretization of the system KU = F, only compute the stiffness matrix (k) from the following process;

$$L\Psi_j = \Psi_{j,x} A_1 + \Psi_{j,y} A_2 + \psi_j \Psi \qquad (3 - 12a)$$

$$K_e = \int_{\Pi_d} \langle L\Psi_1, L\Psi_2, L\Psi_3, .., L\Psi_{Ne} \rangle^T \langle L\Psi_1, L\Psi_2, L\Psi_3, ..., L\Psi_{Ne} \rangle \, d\Pi \qquad (3 - 12b)$$

After computing the stiffness matrix (k) then used the system KU = f to convert into discrete algebraic system for the computations of velocity field (u and v), Pressure (p) and Vorticity (w). In the end chosen the most applicable numerical tool Newton Raphson method that is more convergent iterative technique.

1.1.3.2.1 NEWTON RAPHSON METHOD

This method is mostly known as iterative process and widely employed in the solution of the non – linear equations for single variable initially and followed this technique initially by Burden and Faires [2005]. After that, widely used in the vast fields of the physical problems for single unknowns and after the computer algorithms development, this method is largely extended for more than one unknown thorough the system of linear and non – linear equations. This process is greatly adopted into the CFD packages especially COMSOL MultiPhysics. Through the package, easily handled the various research problems based upon the non – linear equations and controlled the number of iterations up to the required level of accuracy. The general form of single unknown is described as under

$$x^*_{i+1} = x^*_i - \frac{f\left(x^*_i\right)}{f'\left(x^*_i\right)} \qquad i = 0, 1, 2, 3.... \tag{3– 13}$$

The equation (3– 13) can be shifted into the determinant form known as Jacobean that are given as;

$$x^*_{i+1} = x^*_i - J\left(x^*_i\right)^{-1} f\left(x^*_i\right) \qquad i = 0, 1, 2, 3.... \tag{3–14}$$

Whilst, $J(x)^{-1}_i$ is known as inverse matrix of all differentials of unknowns in terms of x and y and the matrix is also called Jacobean matrix that is defined as belew;

$$J(x)^{-1} = \begin{bmatrix} \frac{\partial f_1}{\partial x}(x) & \frac{\partial f_1}{\partial x}(x) \cdots & \frac{\partial f_1}{\partial x}(x) \\ \frac{\partial f_2}{\partial x_1}(x) & \frac{\partial f_2}{\partial x_2}(x) \cdots & \frac{\partial f_2}{\partial x_n}(x) \\ \vdots & \vdots \quad \cdots \quad \vdots & \\ \vdots & \vdots \quad \cdots \quad \vdots & \\ \vdots & \vdots \quad \cdots \quad \vdots & \\ \frac{\partial f_n}{\partial x_1}(x) & \frac{\partial f_n}{\partial x_2}(x) \cdots & \frac{\partial f_n}{\partial x_n}(x) \end{bmatrix}$$

For the computations of all unknowns from the equations (3 – 14), it is necessary to fix or assume the initial guessing for all unknowns so assume as $(0, 0, 0,,,,,,,, 0)$. Further, applied the above process through the equations (3– 1 4).

4.1 DISCUSSIONS OF THE PREDICTED RESULTS

The Discussions is based upon the predicted results taken by the use of the finite element approach with inclusion Galerkin least square residuals. The predicted results are focused on the investigations of the Newtonian and incompressible fluids transport through the various ratios of the backward step duct. The fluids examined on the bases of the different Reynolds number and effects of the ratio in the domain with fixed Reynolds number. The flow patterns observed as streamlines of the velocity, vortex measurement observed in the corners of the domain.

4.1.1 INFLUENCE OF THE REYNOLDS NUMBER ON FLOW PATTERNS OF THE DIFFERENT RATIOS IN THE BACKWARD STEP DUCT.

First, designed the actual domain that is known as backward step duct with necessary initial and boundary conditions at all zones of the duct, mesh structures, streamlines of the velocity, computations of the flow features plots like vortex length and vortex intensity as recirculation flow rate on the bases of the Reynolds number.

In the start, figure – 4.1 described the schematic domain of the research problem that are known as backward step channel with small channel as outlet. In the domain, the parabolic inlet, zero pressure at outlet and Neumann boundary conditions because of the stationary walls are imposed. In the continuity, figure–4.2 descried the finer and extremely refined and structured meshes for both ratios 1:6 and 1:12 of the backward step channel. The finite element triangular structure is chosen with lowest step size 1.3e-03. Figure–4.3(a) described the streamline laminar flow patterns of the velocity and changing various Re's. Startlingly, the very tinny primary eddy is observed at the left silent corner of the expansion channel and due to increasing the Re's the size of the Primary eddy is enhanced and moved towards outlet of the channel and no secondary eddy is appeared at lower Re's (=300). Similarly figure–4.3(b) is altered the flow phenomena, due to increased more Re's, the primary eddy is enhanced more in size and clearly observed in silent corner of the expansion channel and almost occupied the whole area of the core flows. The secondary vortex is also initiated from Re=300 at upper corner of the expansion channel and due to increased Re's (up to 700) the secondary eddy is slowly grows in size at right upper corner of the expansion channel. Another tertiary vortex is also observed at the left lower corner of the backward step duct. Figure – 4.4(a and b) described the streamline patterns for the increased in ratio 1:12 of the backward step channel. Here increased the ratio 1:12 to enhance the size of the expansion portion of the channel. Due to enhance the ratio, both primary and secondary eddies are observed initially (Re = 01) that is not developed in lower ratio (1:6). Also, with increasing the Re's the primary vortex is largely in size is increased towards horizontally and vertically and slowly increased the secondary eddy in size in the corners of the expansion portion of the channel. Consequently, increased more Re's, the primary eddy is clearly observed the enhancement vertically and horizontally at the left silent corner of the expansion portion of the channel but secondary vortex is very too slowly enhanced in size at the upper right corner of the expansion portion of the channel. Subsequently, increased Re's up to 500, the large primary eddy is clearly observed at the silent corner of the expansion channel and completely filled with the large eddy in the whole region of the expansion portion of the channel. And similarly, the secondary eddy is enhanced very slowly in size at the upper right corner of the expansion portion of the channel. Due to increase the ratio 1:6 to 1:12, the computations are increased further up to Reynolds number 1000. Figure–4.5 described the more streamline laminar flow patterns and in these patterns, three different vortices are observed primary at lower corner (main core flow), secondary at upper right corner and tertiary at lower corner of the backward step duct. The computations are started from Re = 700 to 1000. The main core flow primary vortex is greatly observed in

size but the secondary vortex is increased but very slow and tertiary is increased but very too slowly.

4.1.2 INFLUENCE OF THE ASPECT RATIOS ON FIXED REYNOLDS NUMBER

Figure–4.6(a) displays the effect of the increasing ratio 1:6 to 1:12 in the expansion portion of the channel with fixed Re = 01, 200, 300 and 600, In lower ratio (1:6) only primary eddy is observed in left corner but in large ratio (1:12), both tinny eddies (primary and secondary) are visualized in each corner of the expansion portion of the channel at lowest Re's (=01) and further, increased to Reynolds number (200), the primary vortex is increased in both ratios but the size in vortex is higher in the ratio 1:12 to 1:6 and secondary vortex is very too slowly increased in size that are negligible. Figure–4.6(b) also described the streamline patterns with increased more Reynolds number (300 to 600), the primary and secondary vortex is visualized clearly and further increased more but the tertiary vortex is appeared at the lower corner of the backward step duct and increased slowly.

In all streamline flow patterns, it is observed that the vortex size is increased on the enhancement of the Reynolds number but the enhancement is lower in the low ratio (1:6) other than the higher enhancement in higher ratio (1:12) of the backward step duct. Therefore, enhancement is justified in the plots of the recirculation flow rate with function of the increasing Reynolds number. Figure–4.7 described the same enhancement visualized due to increase the Reynolds number and both plots observed the enhancement but visualized the quick linear enhancement observed in the recirculation flow rate for the higher ratio 1:12 of the backward step duct. Further, Figure–4.8 described the plot of the computations of the primary vortex length observed in the streamline laminar flow patterns and clearly visualized that the primary vortex is clearly increased slowly in lower ratio 1:6 and quick increase din plot in the higher ratio 1:12 of the backward step duct. In the last, table – 4.9 and 4.10 described the detail quantitative values of the recirculation flow rate and vortex length in size with different Reynolds numbers.

In this research project, newly computed the empirical equations through the statistical measures as least square regression equations for both ratios of the geometry. These empirical equations are focused on the maximum value of the recirculation flow rate with various Reynolds number that are listed as below;

For ratio 1:6

$$X_{16} = 1.97723e-06\,\mathrm{Re} + 4.3645e-03 \qquad 1 \le \mathrm{Re} \le 600$$

For ratio 1:12

$$X = 1.98797e-06\,\mathrm{Re} + 4.487e-03 \qquad 1 \le \mathrm{Re} \le 1000$$

4.2 SUMMARY

The COMSOL MultiPhysics package is selected for the numerical predictions of the velocity filed and pressure scalar quantity through the governing equations based upon the momentum transport equation with couple of the continuity equations. The Galerkin finite element tool is employed for the discretization of the governing equations with addition of the least square residuals in the shape function. Further, designed the flow features of the velocity field like streamline laminar flow features and others such as recirculation flow rate and vortex reattachment length at different Reynolds number. For the flow features, two ratios 1:6 and 1:12 of the backward step duct are chosen that relates to the large applications of the engineering and industries. The primary vortex at lower left corner and secondary vortex at upper right corner vortex is observed at different Reynolds number but the primary vortex is largely increased and secondary vortex is slowly increased due to increase the Reynolds number. Due to increase the ratio 1:6 to 1:12, the primary vortex is quick appeared and too large eddies observed at each corner of the backward step duct. The same increment of the vortex phenomena is validated in the computations of the recirculation flow rate and vortex length that also appeared the linear and non–linear enhancement. The CFD package results are completely compared the flow patterns with the other flow patterns computed through other packages and other numerical tools.

FIGURES

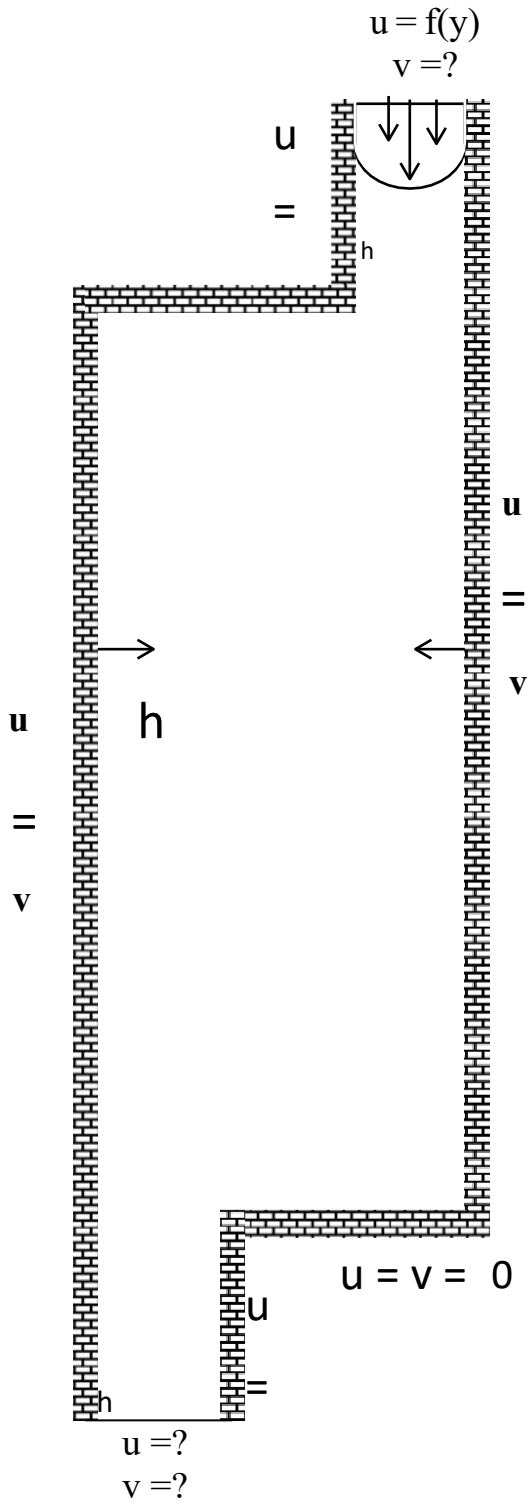

Figure–4.1: Schematic diagram of the two–dimension rectangular backward step duct.

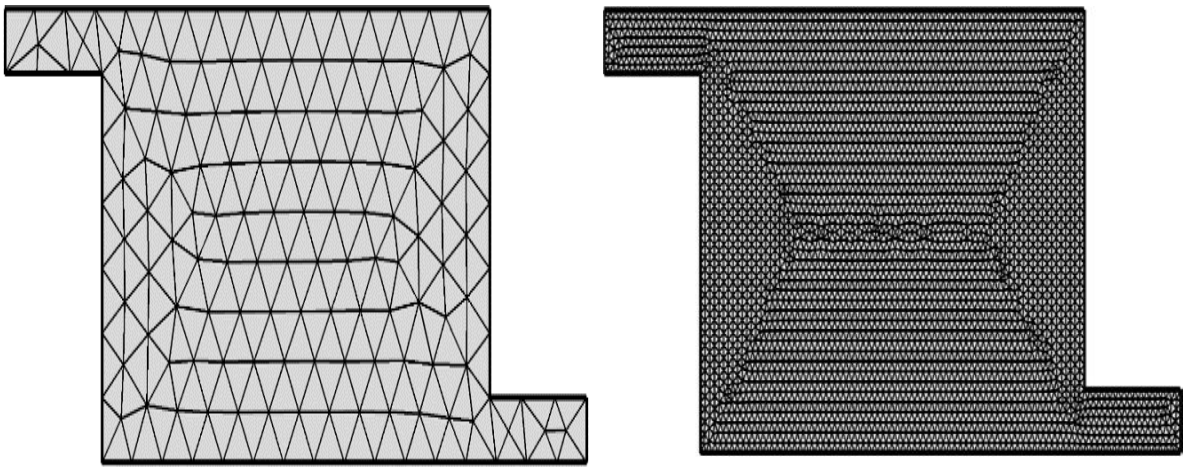

(a)

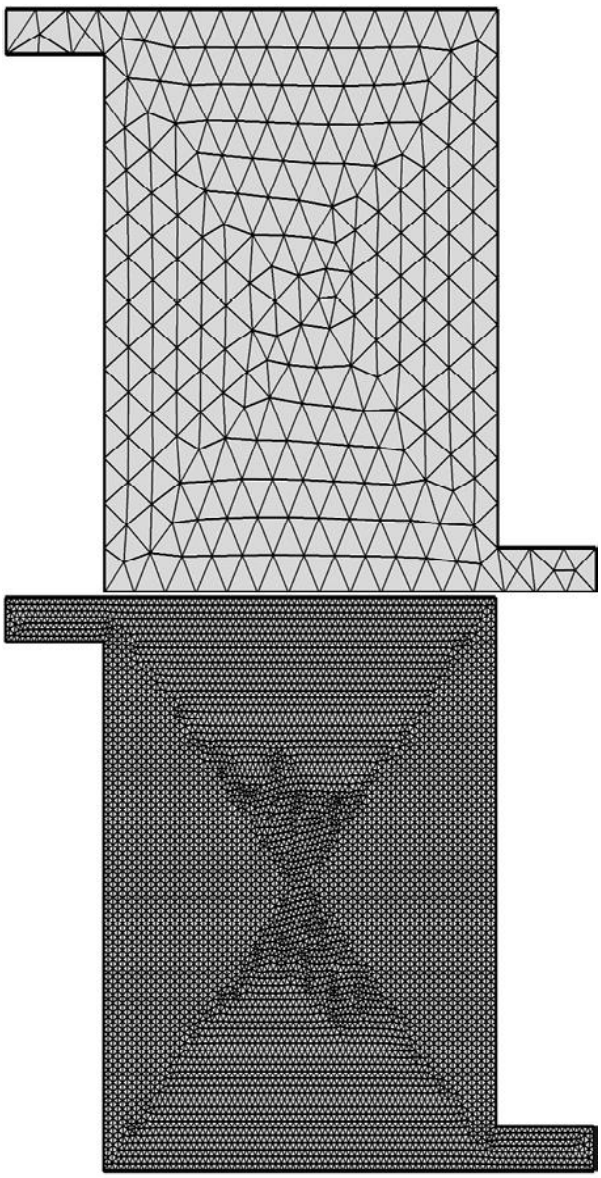

(b)

Figure–4.2: Finer and Extremely fine mesh of the rectangular backward step duct for the ratio (a) 1:6 and (b) 1:12.

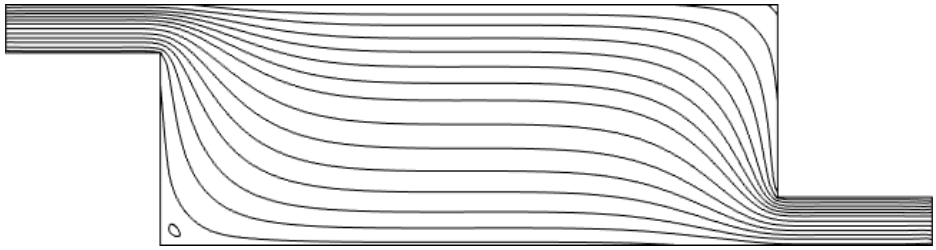

Re = 01

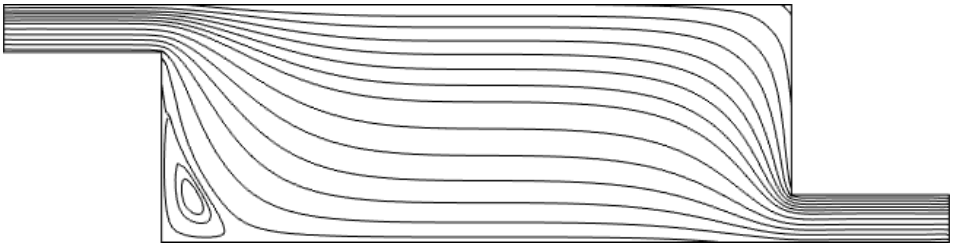

Re = 100

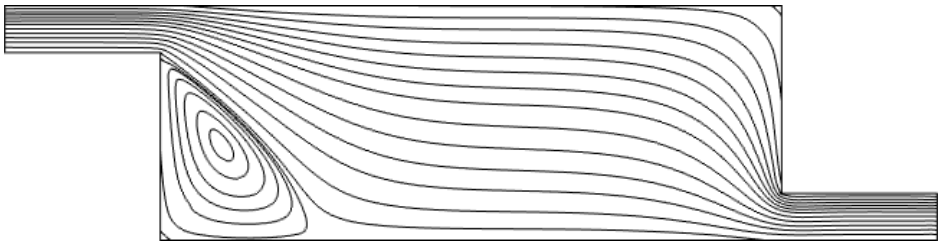

Re = 200

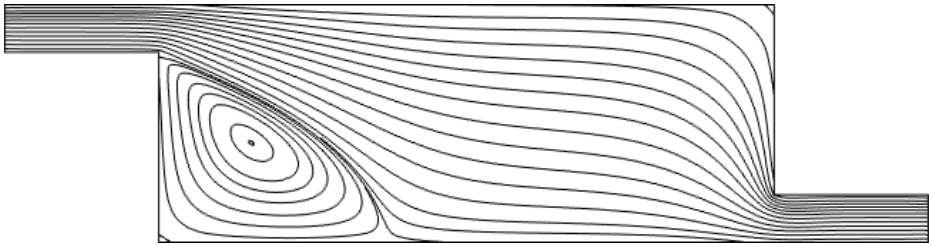

Re = 300

Figure –4.3(a): Streamline Contours of Velocity of the 2 – D backward step duct in a ratio 1:6 ($01 \leq Re \leq 300$)

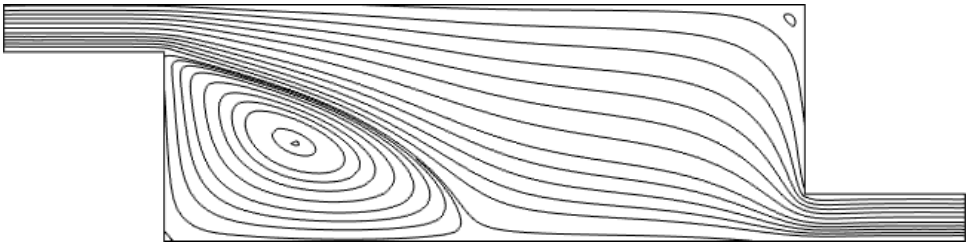

Re = 400

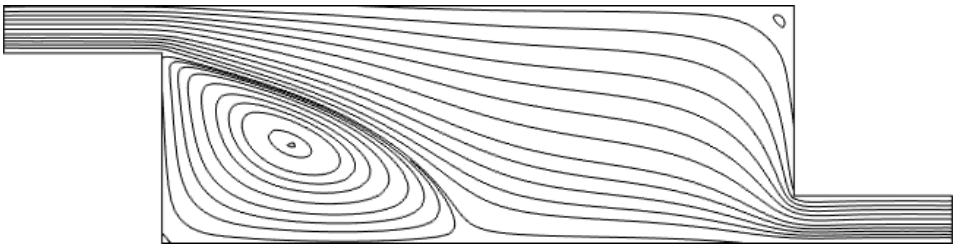

Re = 500

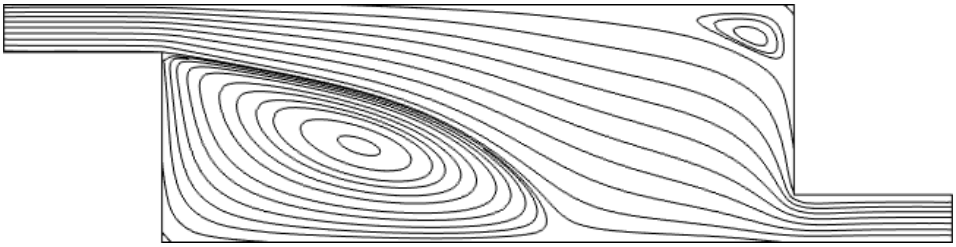

Re = 600

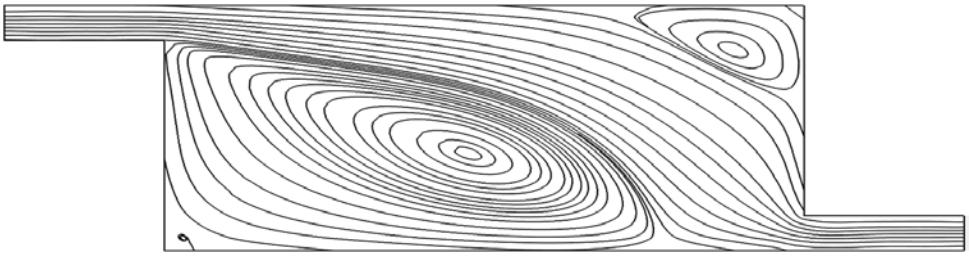

Re = 700

Figure –4.3(b): Streamline Contours of Velocity of the 2 – D backward step duct in a ratio 1:6 ($400 \leq Re \leq 700$)

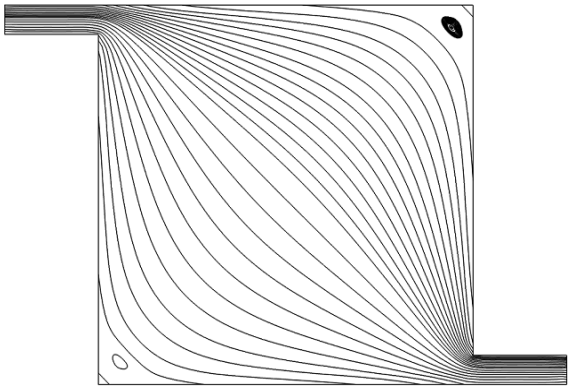

Re = 01

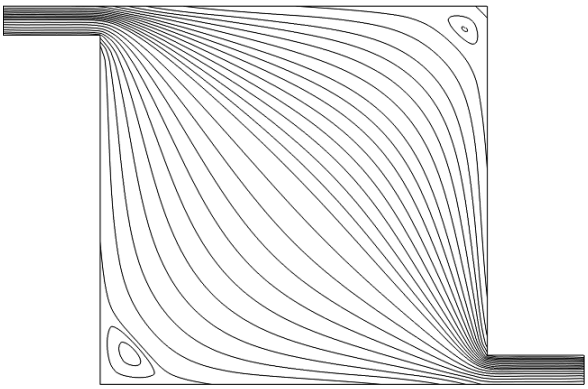

Re = 100

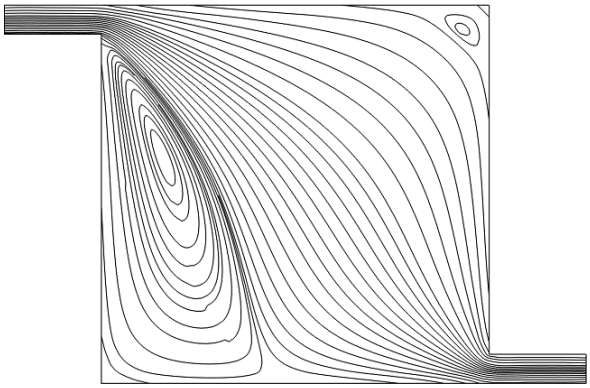

Re = 200

Figure –4.4(a): Streamline Contours of Velocity of the 2 – D backward step duct in a ratio 1:12 ($01 \leq Re \leq 200$)

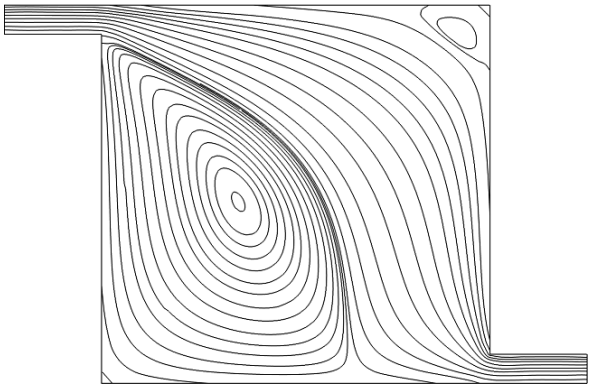

Re = 300

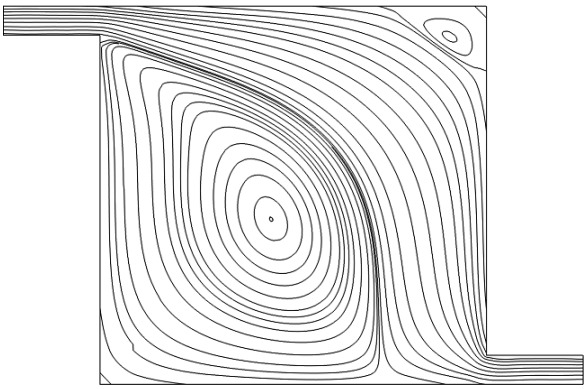

Re = 400

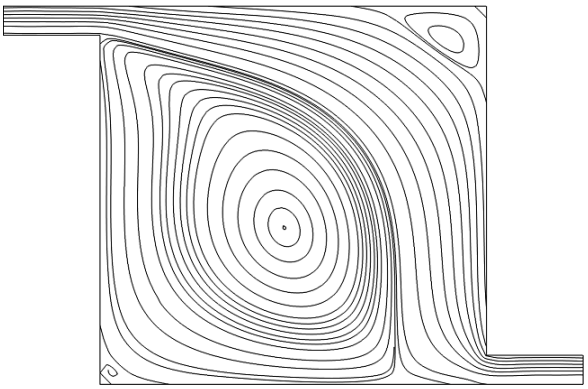

Re = 500

Figure –4.4(b): Streamline Contours of Velocity of the 2 – D backward step duct in a ratio 1:12 ($300 \leq Re \leq 500$).

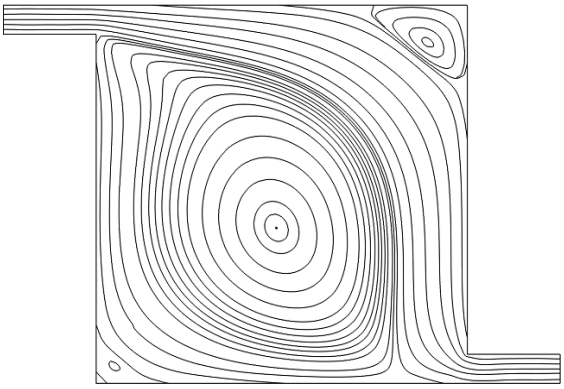

Re = 700

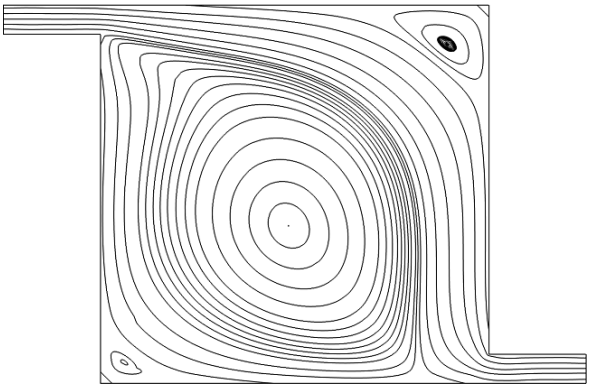

Re = 800

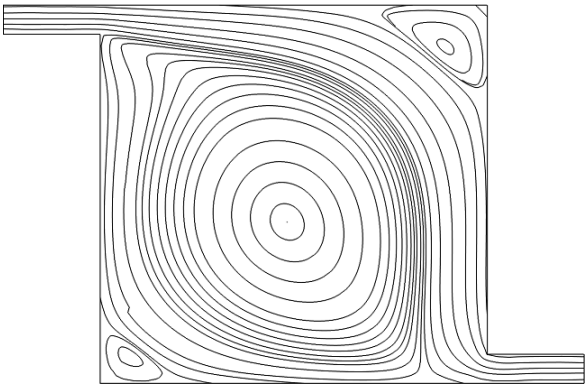

Re = 1000

Figure –4.5: Streamline Contours of Velocity of the 2 – D backward step duct in a ratio 1:12 ($700 \leq Re \leq 1000$).

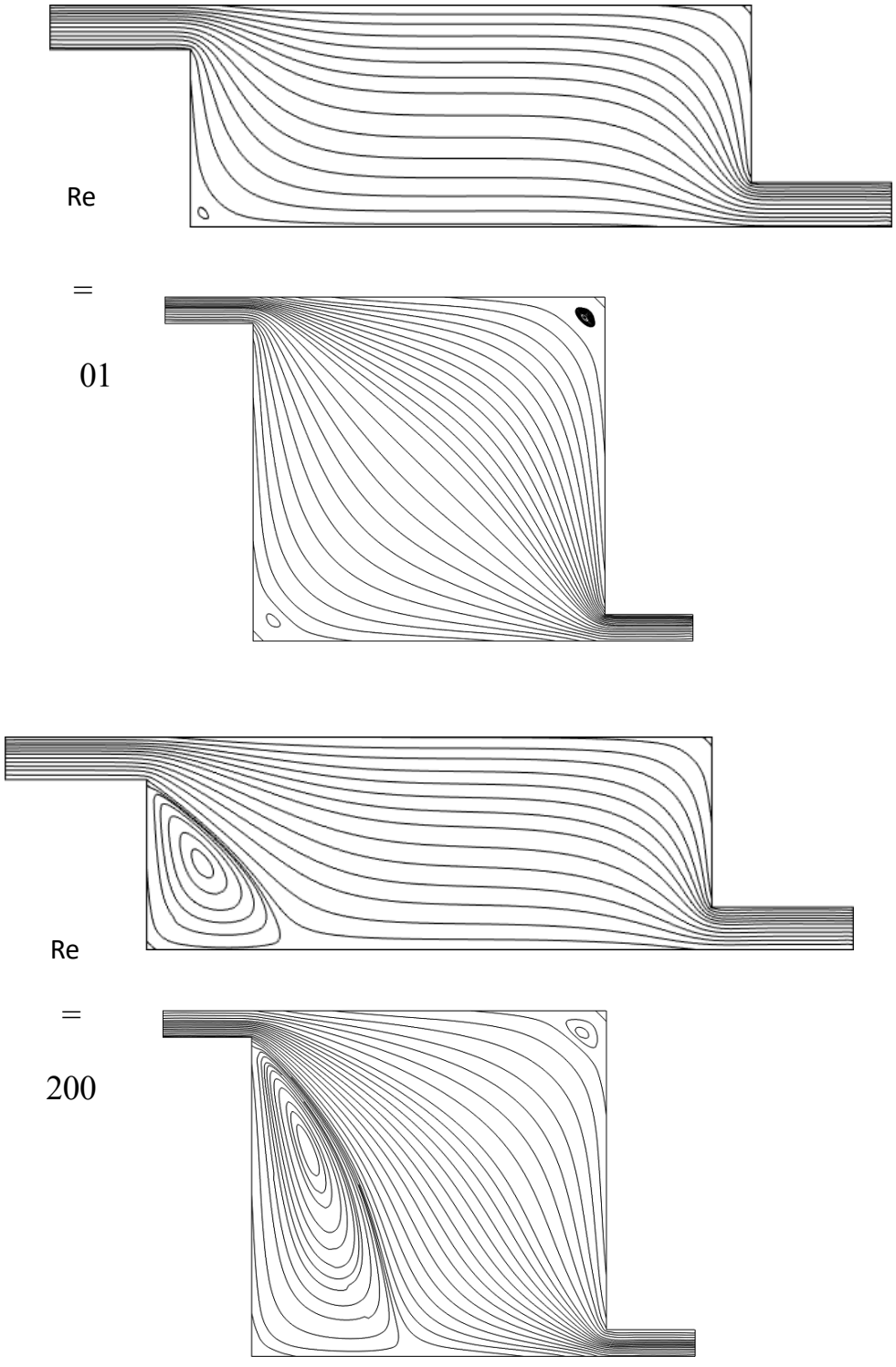

Figure –4.6(a): Streamline Contours of Velocity of the 2 – D backward step duct in a different ratio (1:6 and 1:12) with fixed Re = 01 and 200.

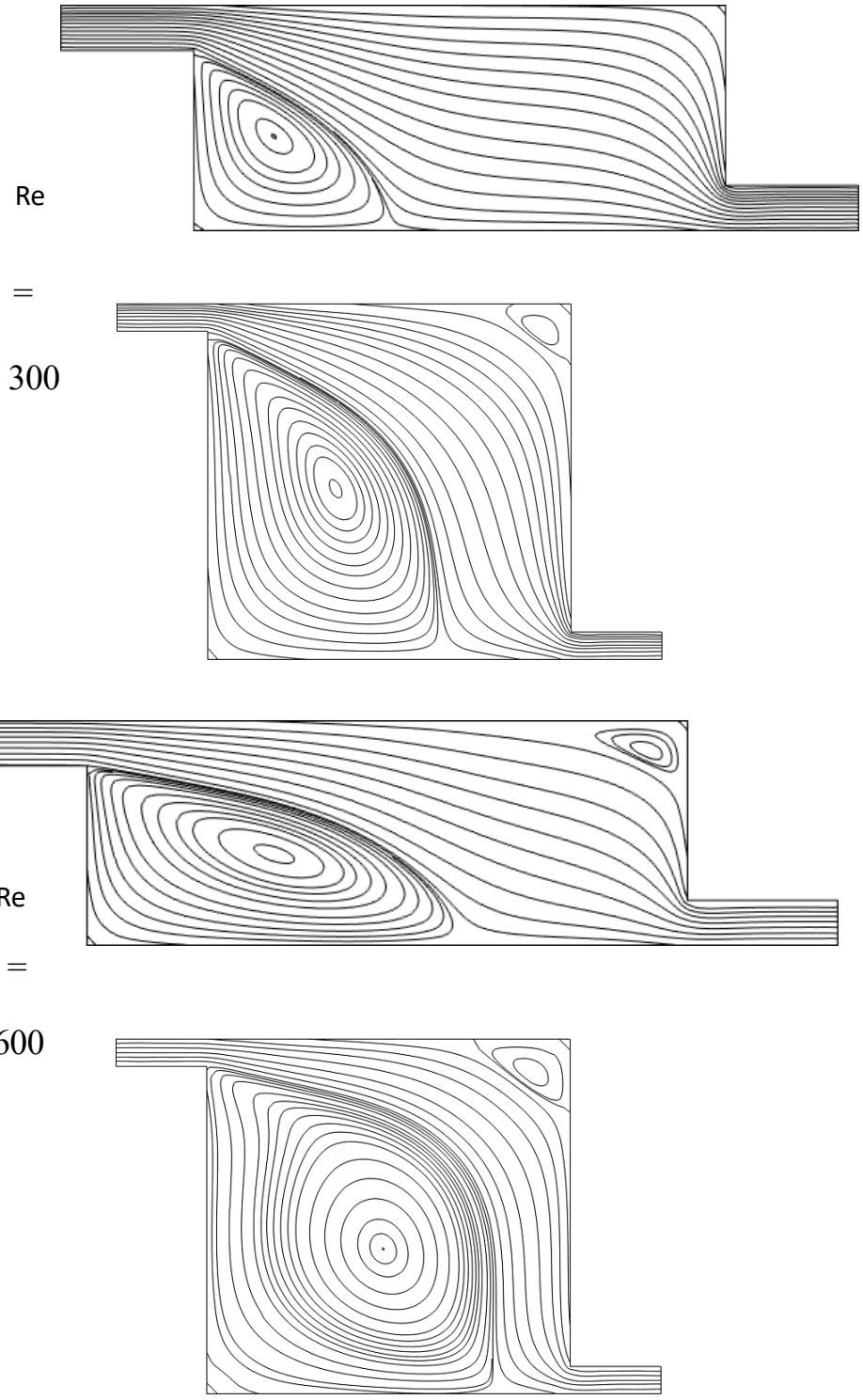

Figure –4.6(b): Streamline Contours of Velocity of the 2 – D backward step duct in a different ratio (1:6 and 1:12) with fixed Re = 300 and 600.

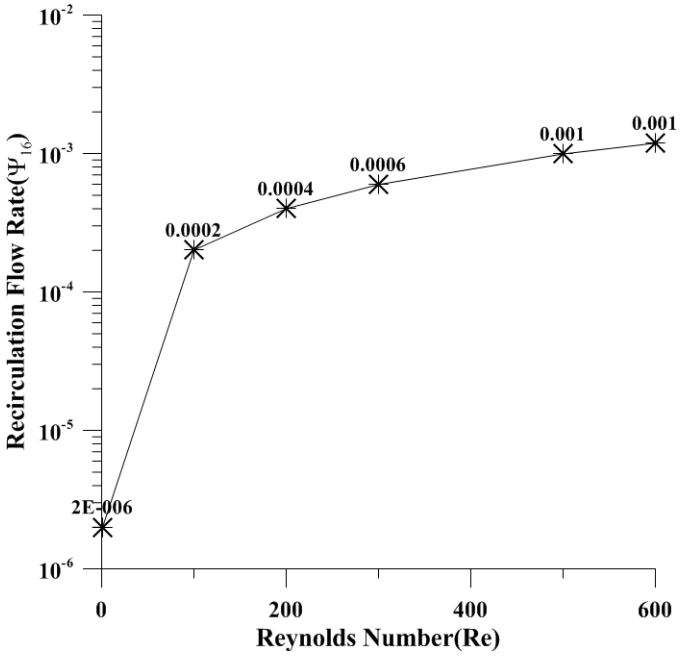

(a)

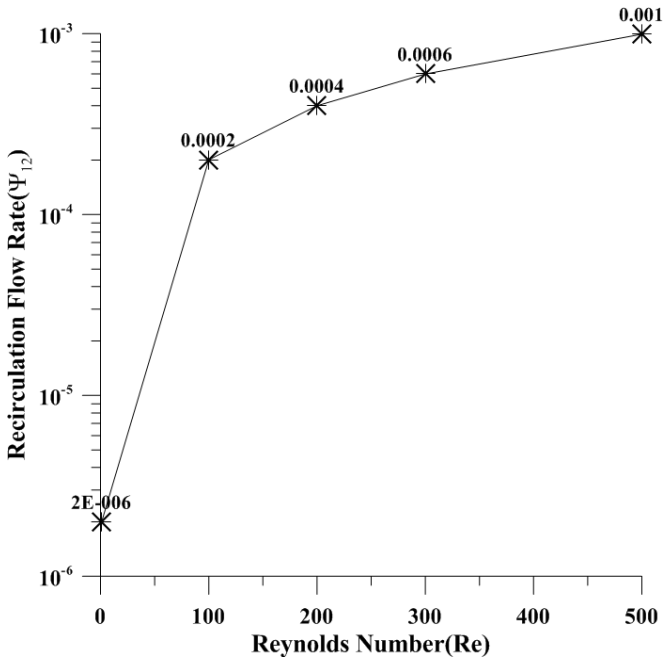

(b)

Figure –4.7(a and b): Recirculation flow rate (Ψ) at various Reynolds numbers (Re) for the 2–D backward step duct in a different ratio (1:6 and 1:12).

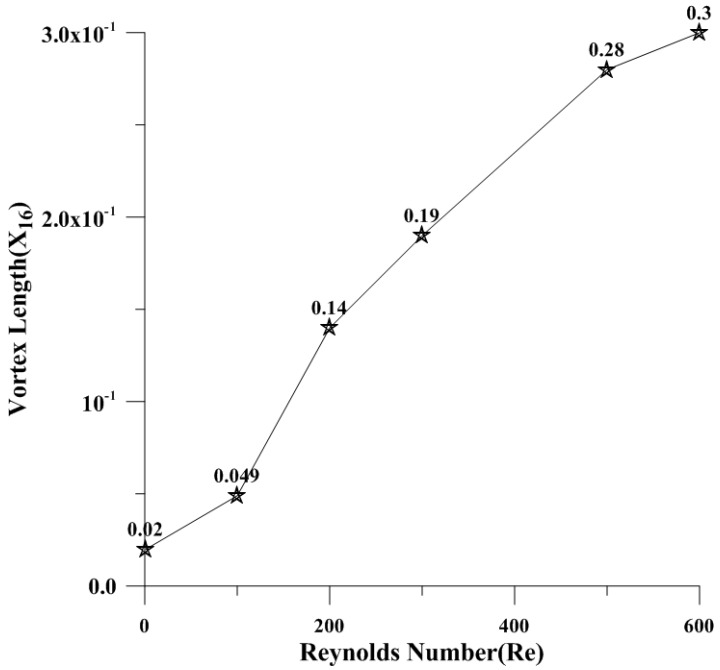

(a)

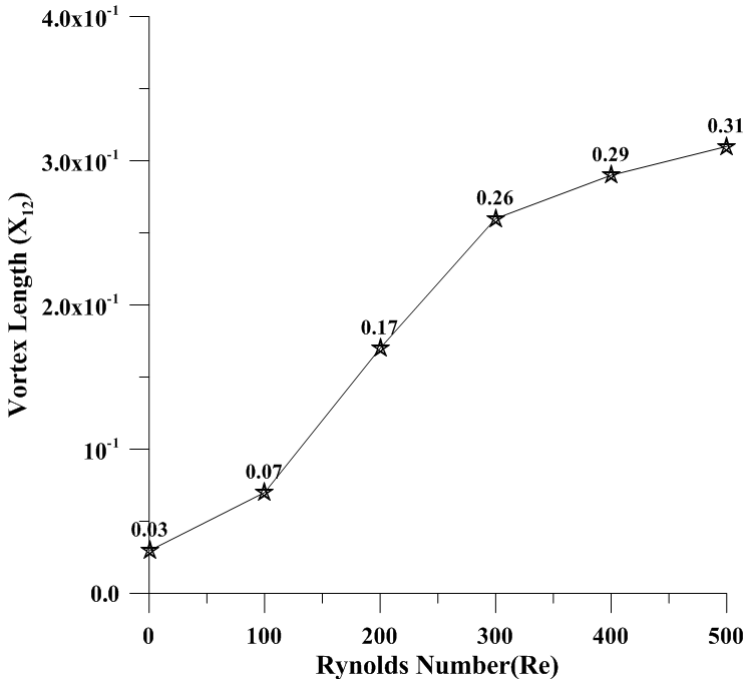

(b)

Figure –4.8(a and b): Vortex length (X) at various Reynolds number (Re)for the 2–D backward step duct in a different ratio (1:6 and 1:12).

Recirculation Flow rate (Ψ)					
Reynolds number (Re)	**Ratio of the domain (1:6)**		**Reynolds number (Re)**	**Ratio of the domain (1 :12)**	
	($\Psi_{1\ min}$)	**($\Psi_{1\ max}$)**		**(Ψ_{2min})**	**(Ψ_{2max})**
01	1.14e-12	2.00e-06	01	2.47e-13	2.00e-06
50	5.25e-11	1.00e-04	50	1.28e-11	1.00e-05
100	7.81e-11	2.01e-04	100	2.74e-11	2.01e-04
200	2.57e-10	4.00e-04	200	8.23e-11	4.00e-04
300	6.81e-9	5.98e-04	300	5.87e-11	5.99e-04
400	3.54e-09	7.96e-04	400	1.99e-10	7.97e-04
500	1.83e-10	1.08e-03	500	4.47e-10	9.94e-04
600	1.03e-08	1.19e-03			

Table–4.9: Minimum and Maximum values of Recirculation flow rate at different Reynolds Number for the ratio 1: 6and 1:12 2–D backward step duct

Vortex Length(X)			
Reynolds number (Re)	**Ratio of the domain (1:6) (X)**	**Reynolds number (Re)**	**Ratio of the domain (1 :12) (X)**
01	0.020	01	0.030
100	0.049	100	0.070
200	0.140	200	0.70
300	0.190	300	0.260
500	0.280	500	0.310
600	0.300		

Table–4.10: Vortex Length (X) at different Reynolds Number for the ratio 1: 6 and 1:2 of 2–D backward step duct.

CONCLUSION AND APPROACHING EXPECTEDWORK

5.1 CONCLUSION

Initially, developed the approximate model called as Galerkin Finite element least square model for two–dimensional research problem. The research problem relates on the transport equation particularly known as momentum equation includes with continuity equation. New technique is chosen here known as Vorticity for the conversion the governing equation into first order system. The first order system is easily discretized through finite element approach and then selected Newton's method for final computations. The problem is chosen the two–dimensional Newtonian fluid flows through two different ratios 1:6 and 1:12 in the backward step duct.

Various flow features are computed and plotted as streamline flow patterns of the velocity, recirculation flow rate and eddy length in size and all focus on the different and increasing Re's. In both ratios of the domain, it is observed that the primary eddy is observed at the lower corner of the backward step duct and very largely enhanced due to increase the Re's initiated from 01 to 600 in the ratio 1:6 of the backward step duct. Also, the secondary eddy is observed at upper right corner of the backward step duct and very slowly enhanced due to increase the Re's. Due to increase the ratio of the backward step duct, in a lower ratio, the small eddies in length are observed and increased and high in

length eddies due to higher ratio at left lower corner and upper right corner of the backward step duct. Due to increase the ratio of the backward step duct on fixed Reynolds number, the vortex phenomena are clearly visualized in the figure – 4.6. At lower Reynolds number (01), the primary and secondary vortex is almost same appeared in the corner of the backward step channel.

In the plots of recirculation flow rate and primary eddy length appeared in the silent corner of the backward step duct is also justified the enhancement in the quantitative values with increasing Re's. The newly developed the Empirical equations that are focused on the quantitative values of the recirculation flow rate with different Re's. The excellent predicted results are obtained and compared with the other numerical results found in literature.

5.2 APPROACHING EXPECTED WORK

The research domain may be extended to observe the behavior of Newtonian in terms of the non – Newtonian fluids. The domain may be extended to fix more than one inlet and also outlet in the backward step channel. It may be fixing the obstacles in the domain of the backward step channel to analyze the fluid flow features and creates the heat and mass transport phenomena.

REFERENCES

Babuska, I., Aziz, K., (1972), Survey lectures on the mathematical foundations of the finite element method. In The Mathematical Foundations of the Finite Element Method with Applications to Partial Differential Equations, (ed. by K. Aziz and I. Babuska), Academic Press, New York.

Battaglia, F., Papadopoulos, G., (2006), "Bifurcation characteristics of flows in rectangular sudden expansion channels. 128, 671 – 679, Journal of Fluids Engineering.

Biswas, B. P. and Chakrabarti, S., (2014), "A Numerical Study on Pressure and Velocity Characteristics of Fluid Passing through a Plain Suddenly Expanded and Contracted Channel", Volume 4, Issue 7, International Journal of Emerging Technology and Advanced Engineering.

Bochev, P., Gunzburger, M., (1994), Analysis of least-squares finite element methods for the Stokes equations, Math. Comp. 63, 479–506.

Bochev, P., Gunzburger, M., (2005), "On least-squares finite element methods for the Poisson equation and their connection to the Dirichlet and Kelvin principles", SIAM J. Numer. Anal. 43, 340–362.

Bochev, P., Gunzburger, (2005), M., "An absolutely stable pressure-Poisson stabilized method for the Stokes equations", SIAM J. Numer. Anal. **42** 1189–1207.

Bochev, P., Gunzburger, M., Compatible least-squares finite element methods, SIAM J. Numer. Anal., to appear.

Camnasio, E., Erpicum, S., Orsi, E., Pirotton, M., Schleiss, A. J. and Dewals, B., (2013), "Coupling between flow and sediment deposition in rectangular shallow reservoirs", 3, 27100, Pavia, Department of Civil Engineering and Architecture, Italy.

Camnasio, E., Erpicum, S., Orsi, E., Pirotton, M., Schleiss, A. J., & Dewals, B. (2014). Coupling between flow and sediment deposition in rectangular shallow reservoirs. Journal of Hydraulic Research, 51(5), 535–547.

Choufi, L., Kettab, A., and Schleiss, A. J. (2014), "Effet de la rugosité du fond d'un réservoir rectangulaire à faible profondeur sur le champ d'écoulement", La Houille Blanche, n° 5, 2014, p. 83-92.

Dewals, B. J., Kantoush, S. A., Erpicum, S., Pirotton, M., & Schleiss, A. J. (2008). Experimental and numerical analysis of flow instabilities in rectangular shallow basins. 8(1), 31–54. Environmental Fluid Mechanics.

Dufresne, M., Dewals, B. J., Erpicum, S., Archambeau, P. and Pirotton, M., (2011), "Numerical Investigation of flow patterns in rectangular shallow reservoirs", vol.5 No.2, pp.247-258, Engineering Applications of Computational Fluid Mechanics.

Kantoush, et al. (2003), "Flow Field Investigation in a Rectangular Shallow Reservoir using UVP, LSPIV and numerical model", pp -129-133, 5th International Symposium on Ultrasonic Doppler Methods for Fluid Mechanics and Fluid Engineering.

Kantoush, S. A., Bollaert, E., & Schleiss, A. J. (2008). Experimental and numerical modelling of sedimentation in a rectangular shallow basin. 23(3), 212–232. International Journal of Sediment Research.

Martijn C. Westhoff, Sébastien E., Pierre A., Michel P. & Benjamin, D., (2017), "Maximum energy dissipation to explain velocity fields in shallow reservoirs", (Online) Journal homepage: http://www.tandfonline.com/loi/tjhr20, Journal of Hydraulic Research.

Memon, et al. (2018), "Finite Volume Simulation of Newtonian Fluids through Combined Converging and Diverging Channel", Vol. 50 (001) 65-72, Sindh Univ. Res. Jour. (Sci. Ser.)

Miranda de, D. A., Rei's dos, Á. M. and Coelho, M. M. L. P., (2018), "Experimental and numerical investigation of flow patterns in shallow rectangular reservoirs with

symmetrically positioned inlet and outlet channels", Versão On-line ISSN 2318-0331, Revista Brasileira de Recursos Hídricos Brazilian Journal of Water Resources

Pozrikidis, C., (2009), Fluid Dynamics: Theory, Computation, and Numerical Simulation, Second Edition. Springer.

Saripalli, P. and Sankaranarayana, K., (2015), "CFD Analysis on Flow through a Resistance Muffler of LCV Diesel Engine", 3(4): 132-145, International Journal of Science, Technology and Society.

Selvadurai, A. P. S., (2013), Transport Phenomena in porous Media, Springer- VerlagBerlin Heidelberg.

Shaikh, H., Shah, S.B., Solangi, M.A. and Baloch, A., (20012), "A Computer Simulation of Flow of Newtonian Fluid through Backward Step Channel", Vol.44 (4) 703-708, Sindh Univ. Res. Jour. (Sci. Ser.)

Shaikh, H., Shah, S. B., Memon, R A. and Baloch, A.., (2017), "Finite element modeling of shear–thinning flow of inelastic non – Newtonian fluid past Expansion Pipe" Vol.49 (1) 69-74, Sindh Univ. Res. Jour. (Sci. Ser.).